



Available online at [scholarcommons.usf.edu/ijis](https://scholarcommons.usf.edu/ijis)

# International Journal of Speleology

Official Journal of Union Internationale de Spéléologie



## Continuous color model as a tool to improve speleothem age model development

Celia Campa-Bousoño <sup>1\*</sup>, Ángel García-Pérez <sup>2</sup>, Ana Moreno <sup>3</sup>, Miguel Iglesias <sup>1</sup>, Hai Cheng <sup>4,5,6</sup>, R. Lawrence Edwards <sup>7</sup>, and Heather Stoll <sup>8</sup>

<sup>1</sup>Department of geology, University of Oviedo, C/Arias de Velasco s/n, 33005, Oviedo, Spain

<sup>2</sup>Department of Psychology, University of Oviedo, Plaza Feijoo s/n, 33005, Oviedo, Spain

<sup>3</sup>Department of Geo-environmental Processes and Global Change, Pyrenean Institute of Ecology-CSIC, Avda. Montañana 1005, 50059 Zaragoza, Spain

<sup>4</sup>Institute of Global Environmental Change, Xi'an Jiaotong University, Xi'an 710049, China

<sup>5</sup>State Key Laboratory of Loess and Quaternary Geology, Institute of Earth Environment, Chinese Academy of Sciences, 710049 Xi'an, China

<sup>6</sup>Key Laboratory of Karst Dynamics, MLR, Institute of Karst Geology, CAGS, Guilin 541004, China

<sup>7</sup>Department of Earth Sciences, University of Minnesota, 116 Church Street SE, Minneapolis, Minnesota 55455, USA

<sup>8</sup>Department of Earth Sciences, ETH Zürich, Sonneggstrasse 5, 8006 Zürich, Switzerland

**Abstract:** Because they can archive a variety of geochemical proxies and be precisely and accurately dated with the U-Th decay series chronometer, stalagmites are widely used for paleoclimate reconstructions. However, limitations in the use of this chronometer arise because U-Th dating is analytically time consuming, expensive, and requires a relatively large sample size. These limitations restrict the number of absolute dates usually obtained, which can result in significant uncertainties in the age model and inhibit the ability to archive high resolution records of environmental variability, particularly in those stalagmites where there are variations in growth rate not constrained by U-Th dates. Here, we explore the relationship between stalagmite color and growth rate. Consequently, we evaluate the use of a simple, practically non-destructive approach to model the age-depth relationship of stalagmites using the sample color to provide a continuous record of growth rate. The method was developed by comparing high-resolution color images with pre-determined U-Th dates along the growth axes of seven stalagmites. The obtained results suggest that prior to dating, a color-derived, continuous growth rate model may be used to identify important changes in growth rate which may aid in the determination of the most efficacious locations for U-Th dating. Further, continuous color-derived interpolations between U-Th derived dates may be superior to traditional linear interpolation methods. Such an approach has the potential to greatly improve a researcher's ability to efficiently choose sampling locations for more precise, albeit laborious and costly, U-Th dating.

**Keywords:** Growth-rate, stalagmite, color, age-modeling

*Received 22 March 2021; Revised 14 September 2021; Accepted 23 September 2021*

**Citation:** Campa-Bousoño, C., García-Pérez, Á., Moreno, A., Cheng, H., Edwards, R.L., Stoll, H., 2021. Continuous color model as tool to improve speleothem age model development. *International Journal of Speleology*, 50(3), 313-326. <https://doi.org/10.5038/1827-806X.50.3.2389>

### INTRODUCTION

Secondary cave carbonate formations, such as stalagmites, are widely used paleoclimate archives. These archives host diverse physical and geochemical proxies useful for reconstructing the local and regional paleoenvironmental conditions that prevailed at the time of their formation (Fairchild & Baker, 2012). Interpretation of the climatic reconstructions is intimately tied to our ability to describe the age evolution, typically constrained by U-Th dating, of the selected speleothems. Exploitation of the U decay series, however, is sample and resource consuming,

with ~200 mg of drilled sample powder and access to modern dating facilities needed for each <sup>230</sup>Th date. Further, there is no standardized procedure for selecting the location of the drill holes where variations in growth rate are recognized only after the initial dates have been obtained.

Continuous measurement of basic physical properties is a routine and rapid check in other paleoclimate archives, like marine or lacustrine sediment cores, and such properties are often used for initial correlation or derivation of age models through orbital tuning (Kemp et al., 2002; Principato, 2005). However, such practices are not a standard

approach in stalagmite studies, which can result in spending more time and resources on U-Th dating than is needed. To circumvent the above-mentioned limitations, some previous studies have focused on the analysis of stalagmite in an effort to tie observational petrographical features to indicators of physical and/or chemical changes in the drip formation of the stalagmites (Dreybrodt, 1999; Frisia et al., 2000; Kaufmann & Dreybrodt, 2004; Frisia, 2014). As such, several studies have suggested that stalagmite coloration may be correlated with growth rate. In particular, it has been suggested that lower calcite saturation during drip formation results in darker color and higher luminescence (Genty & Quinif, 1996; Webster et al., 2007; Vanghi et al., 2019), which has been indicated in annually laminated stalagmites which feature alternating light porous and dark compact layers representing fast and slow growth rates (Treble et al., 2005; Fairchild & Baker, 2012).

In a late Holocene stalagmite from western France, a more rapid growth phase was characterized by lighter color and higher water content in fluid inclusions, than more slowly growing darker calcite (Labuhn et al., 2015). Based on this observation, it is possible that faster growing calcite contains greater density of crystal defects which can be filled with water, conferring a lighter color than defect-poor slower growing calcite. Describing a stalagmite from central China, Tan et al. (2009) found that rapid phases of growth were archived in white sections, intermediate growth rate in grey or grey-yellow sections, and slowest growth rates in dark grey sections of the sample. In addition, it has been shown experimentally that the redness, or red-brown hues, reflect the abundance of organic molecules derived from soils and integrated into the formation's drip water (Chalmin et al., 2013).

Despite the recognition that color variations in stalagmites are well correlated with physical and chemical changes in the speleothem (Cui et al., 2012; Fairchild & Baker, 2012; Hirschev, 2015; Pontes et al., 2020; Kaal et al., 2021), continuous analysis of rapidly quantifiable color has not yet been widely adopted for speleothem study. Here we expand upon previous findings and explore the use of color for providing improved efficacy of sample selection for U-Th dating.

We describe the optimal approach for obtaining continuous color data and investigate the correlation between color and growth rate, as constrained by U-Th dates. We further present the development of a color-based continuous growth rate model for seven Iberian stalagmites which can be used to more effectively choose U-Th sampling locations in other stalagmites. Finally, since some climate indicators have been previously related to the growth rate (Stoll et al., 2013), we also evaluate if there are systematic relationships between stalagmite color and summer insolation and sea surface temperature (SST) by comparing our model with previously published paleoclimatic data.

## MATERIALS AND METHODS

### Samples

Seven calcitic stalagmites were collected from the Iberian Peninsula from four different caves (Fig. 1). The stalagmites cover a wide range in absolute age, growth rate, length, and diameter (Table 1). Identifiers of the samples here follow the naming convention of previous publications on these stalagmites and are thus referred to as: Zerolin, Gloria, Gael, Giovanni, Artemisa, Paz, and Candela (Stoll et al., 2013, Stoll et al., 2015).

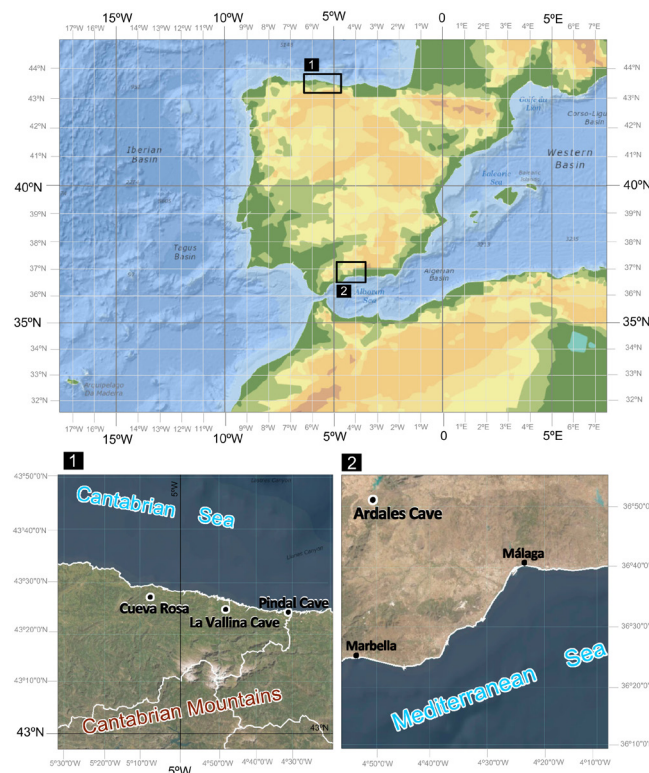


Fig. 1. Location of study sites. The cave sites are situated in Northwestern (1) and Southeastern (2) part of the Iberian Peninsula.

Stalagmites were identically imaged with the exception of Zerolin. This speleothem, showing a very characteristic and detailed lamination, was scanned for a previous study at a higher resolution than the

one used here. At the time of this work, Zerolin had sustained fractures such that images from the previous study are of higher quality than could be obtained for this study.

Table 1. Location, average growth rate, and imaging details for stalagmites investigated.

Stalagmite	Cave name/Location	Coordinate	Image resolution (pixel/inch)	Image creation (year)	Average growth rate ( $\mu\text{m}/\text{yr}$ )
Zerolin	Ardales	36°52'22"N 4°49'44"W	1,200	2016	817
Gloria	La Vallina, Porrúa	43°24'36"N 4°48'24"W	72	2019	4
Gael	La Vallina, Porrúa	43°24'36"N 4°48'24"W	72	2019	18
Giovanni	La Vallina, Porrúa	43°24'36"N 4°48'24"W	72	2019	37
Artemisa	Cueva Rosa, Calabrez	43°26'37"N 5°08'25"W	72	2019	62
Paz	Pindal, Pimiango	43°23'50"N 4°31'58"W	72	2019	28
Candela	Pindal, Pimiango	43°23'50"N 4°31'58"W	72	2019	128

The stalagmites were sampled for color analysis from four different caves on the Iberian Peninsula in 2019 with the exception of Zerolin, which was sampled in 2016. Average growth rates range from 4  $\mu\text{m}/\text{year}$  (Gloria) to 817  $\mu\text{m}/\text{year}$  (Zerolin).

### U-Th chronology

U-Th dates were obtained either at the University of Minnesota or the University of Xi'an Jiaotong using methodology described previously (Shen et al., 2002; Cheng et al., 2013) with ICP-MS (Thermo-Finnigan ELEMENT) or MC-ICP-MS (Thermo-Finnigan Neptune). Details of dates have been previously reported (Stoll et al., 2013, 2015). Results reported here for the first time are given in Supplementary Table S1 (see [Supplementary Information](#) file).

Initial U-Th based age models were determined with two different methods. The first was the use of a simple linear interpolation between two adjacent dates. The second was a more complex model derived from Bchron which use a piecewise linear process to build age models (Haslett & Parnell, 2008; Parnell et al., 2008; Hua et al., 2012). It has been decided to use Bchron due to its methodological advantages such as the ability to extract an ensemble of age models all consistent with the posterior distribution of ages (Hu et al., 2017). The two approaches produced only minor differences in growth rates. Dates derived from simple linear interpolation were used in building the interval and continuous color derived age-depth models and Bchron derived dates were used to validate the continuous color model.

### Stalagmite preparation and image acquisition

Samples were polished for 15 minutes with 320 and 600 grit sandpaper on a wet belt sander and then the surface was wetted directly before scanning. Artemisa, Gloria, Paz, Candela, Gael, and Giovanni were scanned in 2019 with an Epson Perfection V600 Photo at ETH Zürich with automatic color adjustment disabled. A black plastic cover was placed overtop to limit the contribution of contaminating light from outside the scanner. A white paper strip was included in the scanning field for subsequent white balancing. A ruler was also included to provide a reference of scale. Zerolin was scanned in 2016 by an Epson Expression

1640 XL at the University of Oviedo with automatic color adjustment disabled. As this image was acquired outside the scope of this study, the above-mentioned white strip used for white balance was not included in the original scan. Thus, a fragment of Zerolin containing a wide color range was rescanned with the same paper strip in 2019 for white balance. The color range in this section was then used to estimate the color of the entire sample using linear regression (Hössjer, 1995).

ImageJ/Fiji software was used to quantify the color index of each stalagmite (Ferreira & Rasband, 2012) (Fig. 2). To do this, a straight line of one pixel wide was drawn along the growth axis of each stalagmite. In those stalagmites where there was a change of direction in the growth axis, several straight lines were drawn. It was decided to use a line with a very small width because the surfaces of the stalagmites had been previously manipulated for sampling procedures. However, in stalagmites without alterations in their surface, the use of a greater line width could be useful to smooth the artifacts in the color (e.g., porosity, fractures). In order to guarantee the representativeness of the color values, parallel lines were drawn for comparison. Red, green, blue, and grayscale profiles were extracted from an 8-bit RGB encoded image and the white balance was adjusted using an automatic macro for ImageJ/Fiji using the white paper strip which accompanied the stalagmite scans. The original macro was written by Bindokas (2006) and modified by Mascalchi (2014). Finally, color indices of HSV (three-dimensional color representation based on the hue, saturation, and value components) were calculated through the non-linear transformation of the RGB values (Smith, 1978).

### Model development and statistical analysis

All analyses were run with Excel and SPSS (v20, Chicago, IL). In this study significance for all statistical comparisons was defined at  $p \leq 0.05$ .

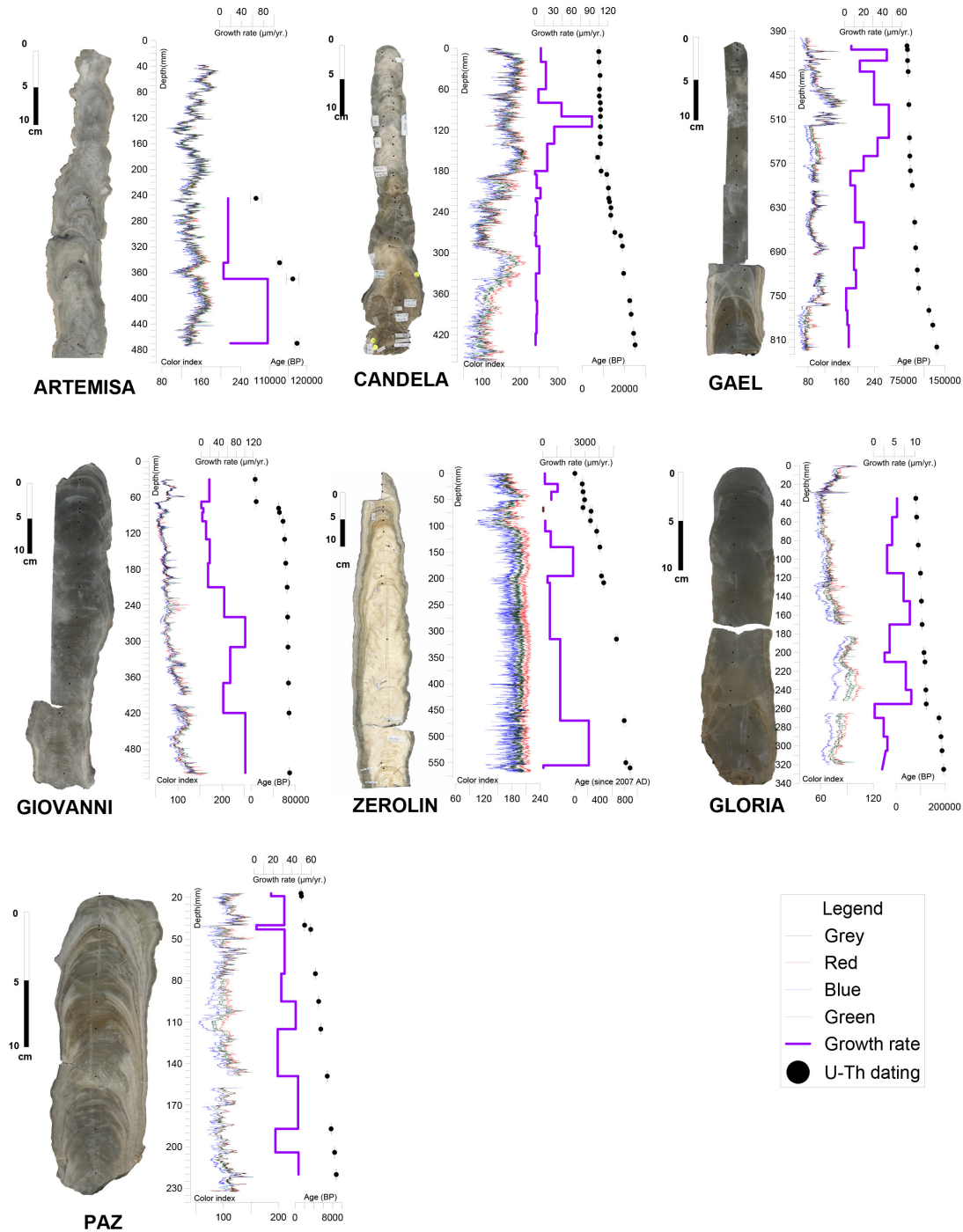


Fig. 2. Longitudinal section images of all stalagmites in this study. Color index values (corresponding-colored lines), growth rate (purple line), absolute value of U-Th dates (black dots), and locations of U-Th dates are shown next to the corresponding samples indicating their respective position along the growth axis (for interpretation of the references to color in this figure and its legend, the reader is referred to the web version of the article).

*Discrete growth rate modelling*

We carried out an exploratory analysis to evaluate the strength of the relationship between color index and growth rate along discrete intervals within the stalagmite (i.e., intervals between U-Th dates), growth rates derived from linear interpolation of the U-Th dates were compared to the average color index in the same interval. Six (linear, exponential, logarithmic, potential, quadratic, and cubic) functions were tested for their ability to describe the relationship and correlation coefficients ( $R^2$ ) were calculated for each function (Supplementary Table S2). The non-parametric Kruskal-Wallis test was then used to test for statistically significant differences between the correlation coefficients. This initial step aims to find

out if a relation between color index and growth rate exists and figure out which mathematical function is the most suitable to explain the above-mentioned correlation.

*Continuous growth rate modeling*

After using discrete interval correlations to identify the most appropriate mathematical function, a continuous color growth rate model was built to describe the entire growth axis of each stalagmite. The model was calibrated using randomly selected U-Th dates, representing 50% of the available data per sample, and the exponential function. Therefore, a single randomized selection of ages was made for each stalagmite. Subsequently, the model was tested

by calculating R2 and the root mean square error (RMSE) using the remaining 50% of the data (Von Gunten et al., 2009). The random selection of the U-Th dates was performed using a random number generator, where each of the U-Th dates had the same probability of being assigned to both the calibration and validation processes of the model. Once the procedure was validated, individual continuous color-age models were built for each stalagmite using all available U-Th dates. Through this second step we intend to put to test the strength of the growth rate and color index relationship.

#### *Correlation of the continuous color model to paleoclimatic events*

Pearson's correlation coefficients were used to evaluate if there was a simple linear relationship between the color index of stalagmites and paleoclimatological proxies such as sea surface temperature or insolation. This analysis can be consulted in the Supplementary Analysis S1 (see [Supplementary Information](#) file).

## RESULTS AND DISCUSSION

### Effects of stalagmite pre-treatment on image quality

Several factors during sample preparation were found to improve color data quality: notably, sanding and wetting. Stalagmites are polycrystalline materials, that is, composed of a three-dimensional mosaic of small, irregular crystals of calcite (Frisia et al., 2000). Reflection can occur when incident rays of light hit a surface, deviate, and return to the medium from which they came at an angle equal to that of the incident light (Hanrahan & Krueger, 1993). When the light strikes an irregular or rough surface, this phenomenon is amplified as diffuse reflection when the incident ray of light is reflected in many angles and many directions (Hanrahan & Krueger, 1993).

Polishing and wetting samples reduces surface roughness thereby reducing diffuse reflection. This is illustrated in Figure 3 where images of Gloria are shown with dry, wet, or wet-polished sample preparation. A dry scan results in large color

variability, shown in Figure 3A, and a nebulous relationship between color index and depth. The color index, instead, appears to trace individual sample pores or indentations made during sample sawing. The wetted sample (Fig. 3B) allows for a more constrained depth – color index relationship but an even clearer picture emerges from the polished *and* wetted surface (Fig. 3C) where depth-color index correlations can be observed at the millimeter scale.

We note that if the same surface is to be drilled for U-Th dating, cleaning of the surface in an ultrasonic bath to remove sample powder generated by polishing, as well as an initial pre-cleaning of the surface by drilling a surface layer and discarding would help reduce the risk of contamination from polishing grit or mixing sample powder of different ages.

The thickness of the stalagmite slab affects the absorption of light (Thomas, 2006) and hence the final color reflectance and quality of the image acquired. A thicker slab has greater absorption and is opaquer, making it more difficult to see internal color variation due to the lack of light transmission (Thomas, 2006). Typically, stalagmite slabs ranging in thickness from 1–2 cm are imaged. While thinner slabs improve light transmission, they can also increase the risk of internal fractures during sawing. Internal fractures oblique to the stalagmite surface generates planes of reflection which produce observations similar to those of variable thickness of the stalagmite slab. This, in turn, generates the artefact of variable color correlated with fracture depth, which itself may also be variable. Indeed, this behavior was observed with an internal fracture in Gloria 260 mm from the tip. In such cases we assumed that the color data are compromised in the affected section and that portion of the stalagmite was not considered in the mathematical models of the stalagmite.

While different physical (density, dimension of the stalagmite, internal fractures, etc.) and environmental (experience/skill of technician) conditions of stalagmite samples individualize their optimum slab thickness, we note that the general aim is to cut the slab as thin as possible. In practice, we have observed that 1 cm thickness is viable for most of the samples.

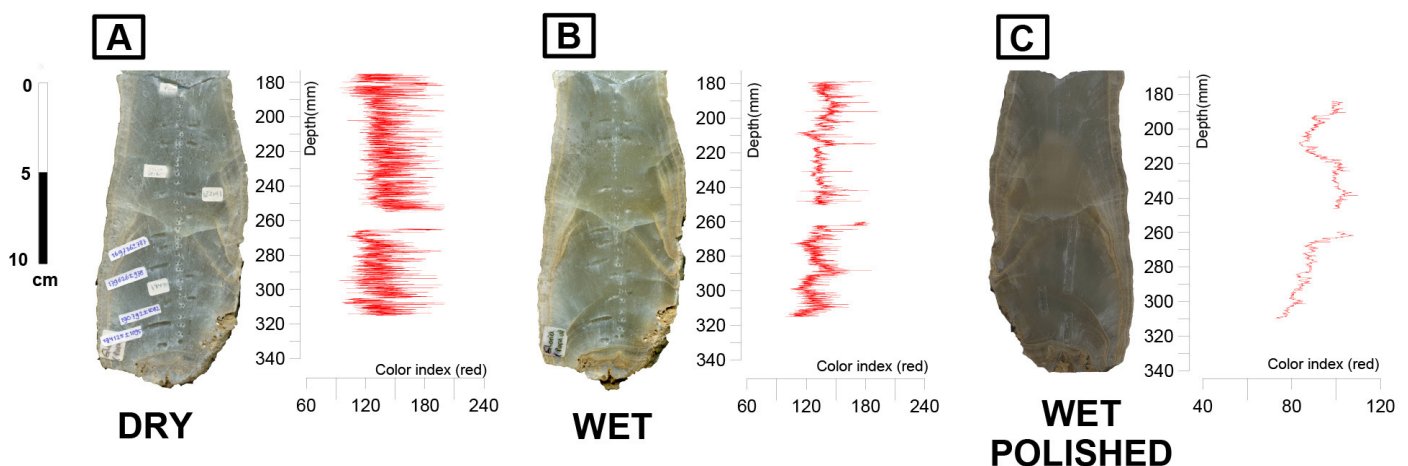


Fig. 3. Images and color index (red) vs depth of dry (A), wetted (B), and polished and wetted (C) longitudinal sections of Gloria. The 8-bit RGB color image profile results in color values (red, green, and blue) ranging between 0 and 255 representing the absence and maximum possible intensity of that color, respectively.

### Relationship between growth rate and coloration: initial exploration

In order to develop a continuous growth rate model based on color, in this section an initial exploration will be carried out on the relationship between color and growth rate using discrete periods. Intervals of average color index and average growth rate between U-Th dated 'tie points' are compared in Figure 4.

All color indices show a direct and positive relationship with growth rate such that higher color indices of white (gray scale), red (red scale), blue (blue scale), and green (green scale) indicate a faster growth rate. Of the seven functions explored, both the exponential (illustrated in Fig. 4) and potential functions are the ones that better describe the relationship between growth rate and color index, and in both cases the correlation of at least three stalagmite models is significant (Supplementary Table S2). Further, color-age models of stalagmites with more U-Th dates appear to show a stronger correlation. In the Gloria stalagmite the relationship between these variables is not clear. This may be due to some of its specific characteristics: like greater thickness of the slab and/or high internal fracturing.

One limitation in this comparison is that growth rates are averaged over discrete, sometimes long, spans of stalagmite growth. In several cases, significant changes in color within these segments suggest that the growth rate may not be constant between U-Th dated points. This appears to be the case for all sections of Artemisa and the first 270 mm of Candela (Fig. 2). If the relationship between growth rate and color is non-linear, then the approach of comparing average color and growth rate may underestimate the true degree of correlation (Goodwin & Leech, 2006). As such, an additional comparison was made using only segments in which the color index has a standard deviation equal to or less than 11 (Supplementary Table S3). This leads to slightly stronger correlations in some stalagmites (Supplementary Table S4) and functions.

It is important to note that very low color indices are indicative of very slow growth phases (less than 3  $\mu\text{m}/\text{year}$ ) or depositional hiatuses. Examples can be seen in Paz, Gloria, or Gael (Fig. 4). In such instances, growth rate seems to have a weaker relationship with color (Supplementary Table S2). These observations may be explained by the presence of undetected or micro hiatuses. To test this hypothesis, sections with

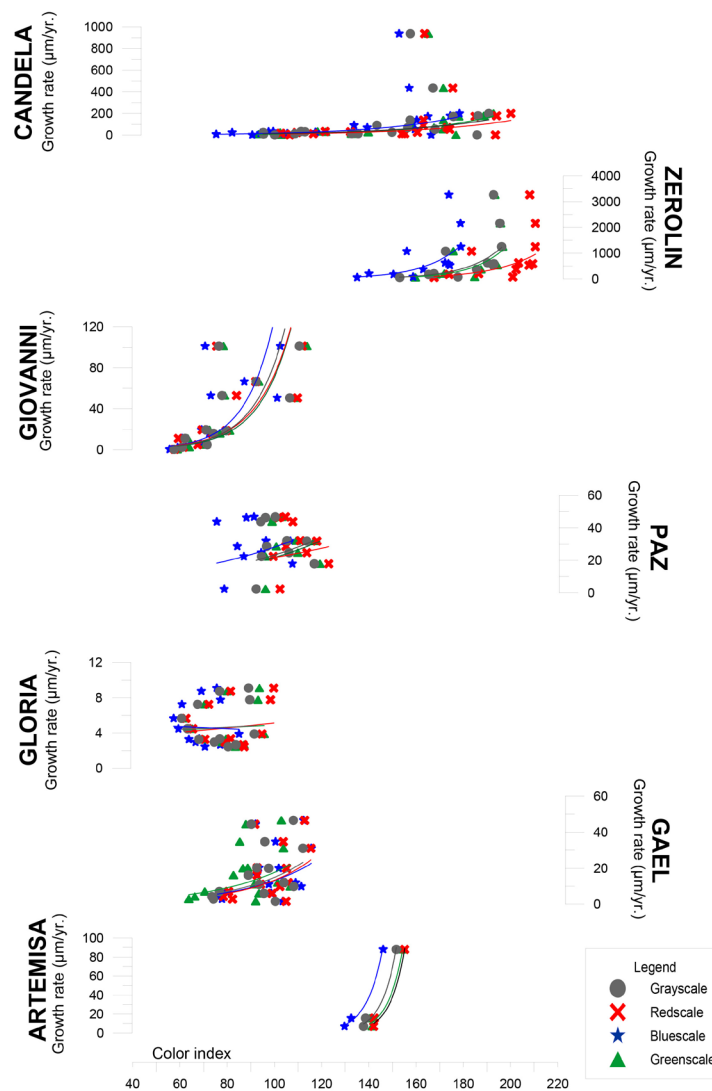


Fig. 4. Average color index (gray, red, blue, and green) in discrete segments vs growth rate for that segment (U-Th derived) for each stalagmite. The line of best fit described by an exponential function is also shown where the color of the line matches the color of the data it describes. Correlation coefficients are presented in the Supplementary Table S2 (for interpretation of the references to color in this figure and its legend, the reader is referred to the web version of the article.) The representativeness of the color indices used was verified by parallel lines through the average in Pearson's correlation ( $r_{xy} = 0.9$ ) for the total of stalagmites and color indices.

extremely slow growth rates (less than 3  $\mu\text{m}/\text{year}$ ) were omitted and the subsequently calculated correlation coefficients improved substantially (Supplementary Table S5).

An estimation of continuous growth rate can be derived from continuous color measurements. In doing so, a choice needs to be made between utilizing the exponential or potential functions, as both describe the correlation between color and growth rate well in discrete sections (Supplementary Table S5). It is reasonable to use an equation based on the exponentiation of the Euler number given that, in the potential equation, a color index values of 0 (black) would indicate an absence of growth. In this way, the potential model would be limited since the presence of a color index (including 0) in a stalagmite will always imply growth, even if that growth is miniscule. However, given the similarity between the exponential and potential functions, it is likely that both functions are equally valid for the construction of a continuous growth rate model at the statistical level. We note that the fact that these data are better fitted with an exponential function implies that lower growth rates will be detected by a greater range in the color index. Therefore, the color index will be more sensitive to slight variations in growth rates, provided there is some growth and it is not a depositional hiatus. Thus, the exponential function was chosen for the continuous growth model.

### Creation of a continuous model of growth rate from stalagmite color

*An exponential fit equation for estimating growth rate from color*

The exponential function was found to best describe the relationship between growth rate and coloration in discrete intervals and was thus used to construct the continuous growth rate models. The proposed model equation is shown in Equation 1.

$$G_c = K \times e^{\text{exp} \times C} \quad (1)$$

where  $G_c$  is the model of growth rate based on color,  $K$  is the coefficient (fixed parameter),  $e$  is the Euler number,  $\text{exp}$  is the exponent free adjustment parameter, and  $C$  is the color index.

The model was tuned in accordance with estimations of the  $K$  and  $\text{exp}$  terms. Based on Koffarnus et al. (2015),  $K$  was calculated by Equation 2:

$$K = \left| \log_{10} \left( \frac{d_t}{a_{\text{final}}} \right) - \log_{10} \left( \frac{d_t}{a_{\text{initial}}} \right) \right| \quad (2)$$

where  $d_t$  is the total distance between the youngest and oldest U-Th dates,  $a_{\text{final}}$  is the oldest U-Th date, and  $a_{\text{initial}}$  is the youngest U-Th date within the dataset. For the calibration-validation exercise,  $a_{\text{final}}$  and  $a_{\text{initial}}$  are the oldest and youngest dates within the calibration data subset, as highlighted in Supplementary Table S6.

Using equation 1 and U-Th dated 'tie points,' the age of all successive points can be found by Equation 3:

$$\text{Year} = \left[ \left[ O_x - \frac{(K_x - K_{x-1})}{\left( \frac{G_c}{1000} \right)} \right] \right] \quad (3)$$

where  $O_x$  is the previous tie-point's date,  $K_x - K_{x-1}$  is the elapsed thickness (mm), and  $G_c$  is the output value from Equation 1.

The exponent free parameter ( $\text{exp}$ ) was iteratively chosen to minimize the difference between U-Th derived ages and color model derived ages using the generalized reduced gradient (grg) nonlinear method implemented via Solver in Excel (Lasdon et al., 1974; Barati, 2013). Therefore, each stalagmite had a unique exponent, which could differ between different stalagmites.

We note that Equations 1 and 3 can be applied for the entire stalagmite, but it cannot predict the youngest date and cannot simulate periods of growth interruption. The model is not applicable for hiatuses as there is no representation in the model for the duration of 'missing' time, and therefore fit parameters will be skewed. In stalagmites with visible growth discontinuity or hiatuses (see Supplementary Table S6), this section is excluded from the model, and it is restarted from the U-Th date where the hiatus ends. Based on previous work (Drysdale et al., 2004; Lewis et al., 2011; Lachniet et al., 2012; Zhao et al., 2015), we have defined depositional hiatuses as occurring in those sections where U-Th derived growth rates are less than 3  $\mu\text{m}/\text{year}$ . All the details regarding the different steps in the execution of the model can be consulted in the [Template Excel Color Model](#).

Optimization of the  $\text{exp}$  and  $K$  terms allows for the creation of a unique set of equations (from Eq. 1 and 2) which correlate color to growth rate for each stalagmite. The color model derived ages are generally within 2SD of the analytical uncertainty for the adjacent U-Th derived dates. The average deviation between modeled and measured age is 2.21% and is no more than 5.67% for any case with the exception of Zerolin (Table 2). The young age of Zerolin, coupled with the greater analytical uncertainty on the U-Th ages as well as blank Th contribution, leads to higher deviations of up to  $\approx 35\%$  in the case of two U-Th dates. However, the difference between the measured and modeled age is still less than 60 years and some points are also considered outliers in the Bchron chronology. Deviations in the model could reflect hiatuses or micro-hiatuses which are not visually recognized and therefore not appropriately managed.

The model was initially run using a randomly selected 50% of the available U-Th dates (calibration) and subsequently validated using the remaining 50% of the dates (validation). This was applied to those stalagmites that had at least a total of eight U-Th dates (all stalagmites except Artemisa). Table 2 shows that the model run with 50% of the U-Th data describes the remaining data well. Using the color-based equation to interpolate between all U-Th ages yields an age model which is expected to be more sensitive to actual growth rates in the speleothem than a simple linear interpolation or Bchron fit (e.g., Fig. 5).

Furthermore, this model can also help us to identify (along with other indicators) outliers. For instance, in the upper section of Zerolin there are several dates that can exhibit issues (i.e., age inversions) according to the age model based on linear interpolation. With the available information, it is hard to determine which of those dates are outliers. However, according to the trend of the age model based on color, one of the possible dates that could be considered an outlier is the U-Th date in the 72 mm, which also has a low  $^{230}\text{Th}/^{232}\text{Th}$  (Supplementary Table S1). Additionally, it is important to note that like Bchron, in the color model it is not necessary to remove this kind of data to estimate the age model.

Further, the observation that all RGB indices and the grayscale indices show a very high fit suggests that each would be equally valid to produce the color age models. However, the red color index works slightly better for some stalagmites (e.g., Paz, Gael, and Giovanni) (Table 2), so models based on red color index will be used in subsequent analyses. An important aspect to note is that the selection of the color index for the construction of the age model must

consider the existing colors in each stalagmite. For instance, in the age models based on the red color index in Figure 5, Candela between mm 100 and 180 does not have a good fit to U-Th dates. However, in Supplementary Figures S1, S2, and S3, it can be noticed that the fit improves remarkably (these aspects can also be observed in the RMSE of Table 2). This may be due to the presence of a bluish-green color in this section ( $\approx$ oceanus, R = 144, G = 172, B = 170), which the red channel underestimates. This finding highlights the relevance of properly selecting the color channel for each stalagmite, since each channel emphasizes the intensity of some colors rather than others. On the other hand, Figure 5 also shows a poor adjustment of the Gael model between 500 and 600 mm. We hypothesize that the inadequate fitting could be due to the presence of a fracture in this section that coincides with the maximum values in the color index, and therefore in the growth rate (Fig. 2). This could lead to an underestimation of the growth rate in this section and therefore to a poor fit of the age model based on color. That highlights the importance of the sample preparation and especially an initial scan of the stalagmites before altering their surface.

Table 2. R2, RMSE, and average deviation (between estimated and empirical dates) for each color model.

Name	Colorscale	All dates			Calibration			Validation		
		R <sup>2</sup>	RMSE (yr)	% deviation in age	R <sup>2</sup>	RMSE (yr)	% deviation in age	R <sup>2</sup>	RMSE (yr)	% deviation in age
Paz	Grey	>0.99**	169	3.92	>0.99**	65	3.26	>0.99**	197	5.87
	Red	>0.99**	164	3.67	>0.99**	81	3.37	>0.99**	143	4.12
	Blue	0.99**	245	5.67	>0.99**	93	3.64	>0.99**	292	8.55
	Green	>0.99**	168	4.23	>0.99**	67	3.20	>0.99**	193	5.59
Zerolin	Grey	0.99**	35	11.42	0.99**	16	18.91	>0.99**	59	12.83
	Red	0.98**	37	10.17	0.99**	13	16.44	0.98**	51	11.50
	Blue	0.98**	37	13.11	0.99**	18	20.20	0.98**	30	14.01
	Green	0.98**	43	12.68	0.99**	17	19.97	0.99**	54	11.31
Artemisa	Grey	0.77	1,131	0.81	-	-	-	-	-	-
	Red	0.75	1,186	0.85	-	-	-	-	-	-
	Blue	0.81	1,005	0.73	-	-	-	-	-	-
	Green	0.77	1,109	0.82	-	-	-	-	-	-
Candela	Grey	>0.99**	428	2.34	>0.99**	455	2.44	0.99**	400	2.02
	Red	0.99**	571	3.87	>0.99**	574	4.06	0.99**	570	3.05
	Blue	>0.99**	434	2.35	>0.99**	460	2.19	>0.99**	330	2.70
	Green	>0.99**	391	2.01	>0.99**	415	2.05	>0.99**	388	1.71
Gael	Grey	0.99**	2,845	2.39	0.97**	588	1.17	>0.99**	1,934	1.90
	Red	0.99**	1,625	1.43	0.98**	453	0.87	>0.99**	1,968	1.92
	Blue	0.99**	2,223	1.91	0.94*	759	1.52	>0.99**	2,538	2.28
	Green	0.99**	1,807	1.63	0.97**	573	1.12	0.99**	2,112	2.03
Gloria	Grey	>0.99**	1,979	1.67	>0.99**	2,255	1.92	0.99*	1,776	1.51
	Red	>0.99**	2,144	1.79	>0.99**	2,408	2.07	0.99*	2,021	1.74
	Blue	>0.99**	1,921	1.60	>0.99**	2,287	1.92	0.99*	1,379	1.29
	Green	>0.99**	1,950	1.58	>0.99**	2,183	1.79	0.99*	1,802	1.51
Giovanni	Grey	>0.99**	888	1.96	0.99**	297	1.30	>0.99**	1,020	2.74
	Red	>0.99**	829	1.76	>0.99**	275	1.20	>0.99**	978	2.45
	Blue	>0.99**	1,212	2.02	>0.99**	482	1.95	>0.99**	1,162	3.22
	Green	>0.99**	885	1.94	>0.99**	288	1.26	>0.99**	1,035	2.75

Dates used for calibration and validation are provided in Supplementary Table S6.

\*p < 0.05; \*\*p < 0.01. Degree freedom were considered in this analysis.

It has been observed that all color indices of the RGB scale, and the gray scale, could be useful and effective in predicting the growth rate, thus highlighting the importance of the variation in the intensity of these color channels. In order to explore what other color characteristics may be related to growth rate, an HSV-based color model was also built (Supplementary Table S7). The H and S parameters, corresponding to hue and color saturation, are not strongly correlated with growth rate (Supplementary Table S8). In addition, both H and S index models produce growth rates which are unrealistic (e.g.,  $>1,020 \mu\text{m}/\text{year}$ ). Furthermore,

that the H parameter is not strongly associated to the growth rate is expected, since there are other factors not dependent on the growth rate that are related to the stalagmite hue (e.g., red-brown hue in stalagmites associated with organic matter). On the other hand, as expected, parameter V, which corresponds to the amplitude of the light, or brightness of the stalagmite, has a similar, albeit slightly weaker, correlation to that of the RGB or greyscale models. Taken together, these results confirm that the black-white (or intensity in each color channel) axis is the factor that best predicts variations in the growth rate of stalagmites.

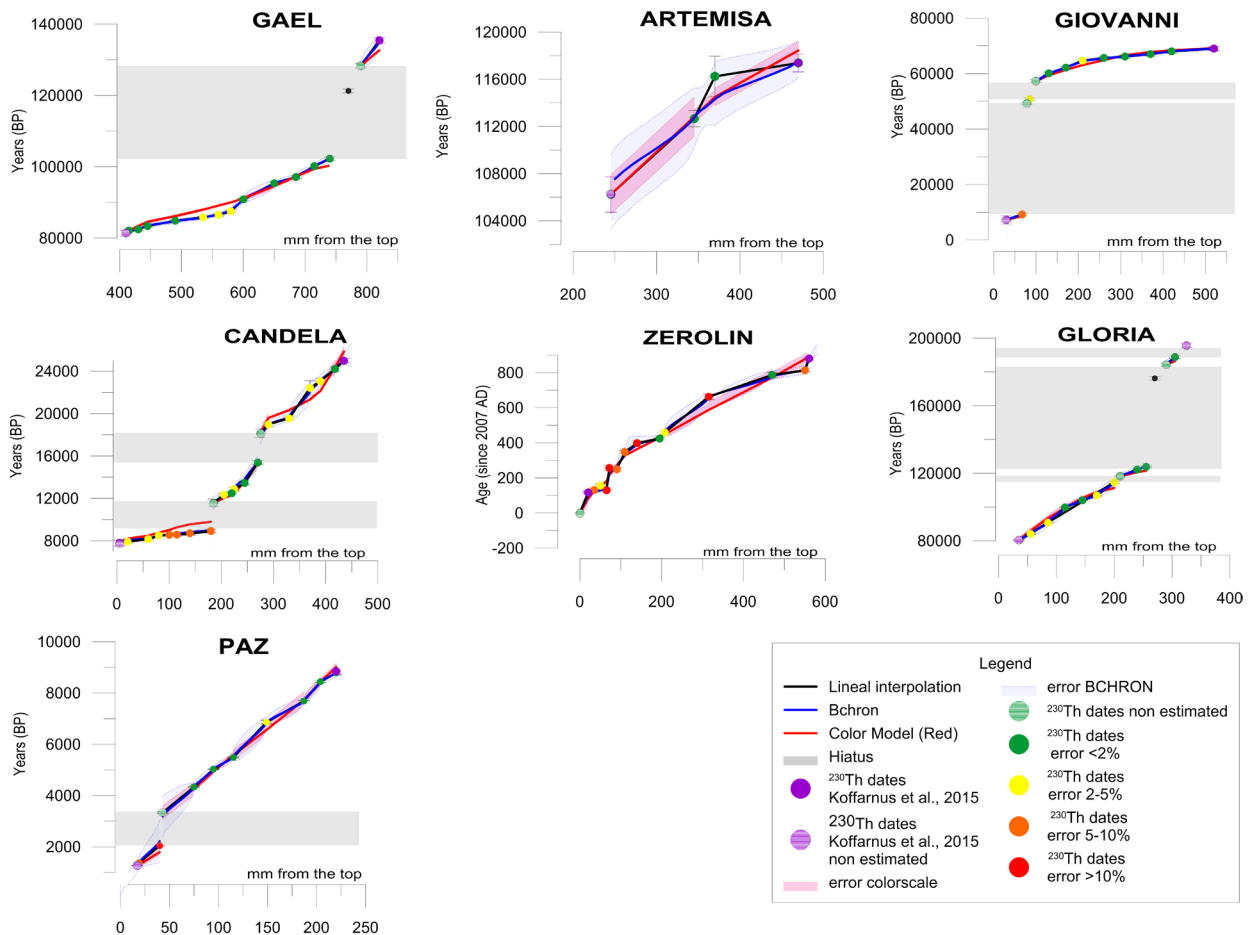


Fig. 5. Comparison of the age model, based on the red color index, with the linear interpolation of the U-Th dates, and the age model constructed by Bchron. The U-Th dates with which the coefficient was calculated are represented in purple. Non-estimated (tie-point) U-Th dates are represented by a hatched circle. Warmer colors in the U-Th dates represent a greater deviation from the modeled age. Figures from the age models based on the gray, blue, and green color indices are available in Supplementary Information (Figs S1–S3).

Finally, considering some of the previous results, there are strategic aspects, which should be taken into consideration in order to achieve an adequate functioning of the model. First, to guarantee a good quality in the extraction of the stalagmite color, the stalagmite must be properly prepared (i.e., polished, wetted, etc.) and must be scanned before carrying out other types of manipulations (e.g., drilling). Second, it is important to select the appropriate color channel based on the predominant colors in the stalagmite. Third, a minimum of three dates is necessary to run the model, since the youngest date is not estimated. However, as in other age models, a greater number of dates will improve the model. Finally, as in other age models, it is also essential to detect whether the stalagmite presents relevant depositional hiatuses.

#### *Is there a unique relationship between color and growth rate for all stalagmites?*

We find that the exponential parameter ( $exp$ ) best describing the relationship between color index and growth rate is slightly different for each of the 7 stalagmites examined (Fig. 6 and Table 3). In part, some differences are to be expected due to variable thicknesses of stalagmite slabs and potential differences in the quality of polish. In addition, Zerolin was scanned on a different system and without a direct white balance, which may lead to additional uncertainties in the quantification of its color. However, there are still variations in the exponential parameter among the 5 stalagmites of similar thickness (17–22 mm) as well as among highly polished stalagmites, suggesting that variation in

the exponential parameter is not exclusively caused by sample preparation. Within this small dataset, there is no clear correlation between the exponential

parameter and the cave location, the average growth rate, or the average Mg/Ca ratio of the stalagmite (Table 3).

Table 3. Coefficient and exponent of each stalagmite model built with the red color index along with its corresponding  $R^2$ , RMSE, and other characteristics.

Stalagmite name	Coefficient (Eq. 2)	Exponent (grg nonlinear)	RMSE	RMSE exp 0.036	Slab thickness (mm)**	Max-Min* diameter (cm)	Polish level (1-4)**	Average* Mg/Ca
Zerolin	0.876	0.033x	35	224	20	4-10	3	8
Gloria	0.386	0.036x	1,719	1,719	35	6-7	1	14.5
Gael	0.221	0.044x	1,465	13,214	17	7.5-8.5	4	12
Giovanni	0.978	0.042x	727	4,180	48	8-11	1	2.5
Artemisa	0.043	0.042x	1,027	11,168	22	4-8	1	3
Paz	0.840	0.034x	148	554	19	6-6.5	2	4
Candela	0.528	0.029x	528	1,634	17	4-8.5	3	1.5

\*The physical and chemical characteristics are: the maximum and minimum of the stalagmites diameter and the average Mg/Ca ratio.

\*\*Stalagmite preparation information is also shown, such as the thickness of the stalagmite when it was cut and its level of polish, which varies from 1 to 4 (1 being poorly polished and 4 highly polished).

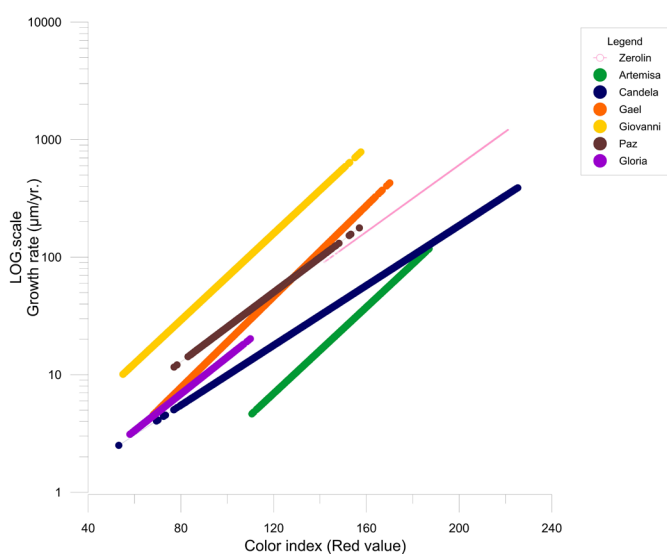


Fig. 6. Red color index (in logarithmic scale) of each stalagmite versus its associated growth rates (derived from the application of Eq. 1). Different slopes reflect different exponents ( $exp$ ) terms in the Eq. 1 and 3 (for interpretation of the references to color in this figure and its legend, the reader is referred to the web version of the article).

The absence of a unique relationship between color and growth rate suggests some limitation in the precision with which color can estimate the growth rate of stalagmites prior to U-Th dating. By averaging  $exp$  terms from the models of each stalagmite, RMSE is increased by as much as 10-fold (Table 3). Despite the uncertainty, the use of this value can provide a useful constraint on the growth rate and duration of a growth phase before dating. On the other hand, for our stalagmite population (using same  $exp$ ), growth rates of less than 5  $\mu\text{m}/\text{year}$  do not exceed a red index of 110. In the case of growth rates between 5 and 100  $\mu\text{m}/\text{year}$ , the maximum and minimum red color index was found to 180 and 70, respectively. Finally, for growth rates greater than 300  $\mu\text{m}/\text{year}$ , the minimum color index was 160. As there appears to be no unambiguous relationship between color and growth rate in the stalagmite population, these examples should be taken with caution.

An important limitation is that, in some cases, the presence of unrecognized growth stops could contribute to an inference with slower growth rates,

since the apparent growth of the stalagmite does not correspond to actual growth because hiatuses are not captured by color. As such, the actual growth rate would be faster than that predicted by the age model based on color index. Regardless, dealing with hiatuses is a widespread challenge in age modeling.

#### Growth rate variability and optimization of location for U-Th dating

A comparison of growth rates calculated by Bchron, and those calculated from color index (Fig. 7), suggests that the length scale of variation from the color index model is much shorter than the spacing of U-Th dates in many samples. Hence, the estimation of a continuous growth rate based on the color index could improve the estimation of growth rates in discrete periods obtained from software such as Bchron.

The variation in the growth rate of the color model also highlights that the current location and number of U-Th dates may have been inefficiently distributed. For instance, it is evident that Artemisa needs more data (currently only has four U-Th dates), and according to the color model for Artemisa the dating density should be at least doubled to accurately date the transitions between sections of variable growth rates to ensure interpolation of ages between dated points is accurate. Although, the opposite situation can also be observed: on Candela, from 370 mm to the base, more dates than necessary have been made to constrain the relevant variation in the growth rate. Even in stalagmites with a high density of dated points, the color-growth rate model suggests that the positioning of these points in several cases was not adequate to accurately detect growth rate variations. For example, in the Gael stalagmite, dating was performed at the abrupt maximum of growth rate (490 mm), which generates an average that does not accurately capture the growth acceleration (Fig. 7). This is significant since variations in the color index can help guiding the selection of dating locations. We note that perhaps the most interesting places to date are those where large changes in color index occur. An example of this is illustrated in Figure 8. Finally, it is interesting to note that since the partitioning

of some trace elements is proposed to be sensitive to growth rate (Tesoriero & Pankow, 1996) a more detailed knowledge of growth rate variability

provided by color indices may also be a valuable asset in the accurate interpretation of geochemical records.

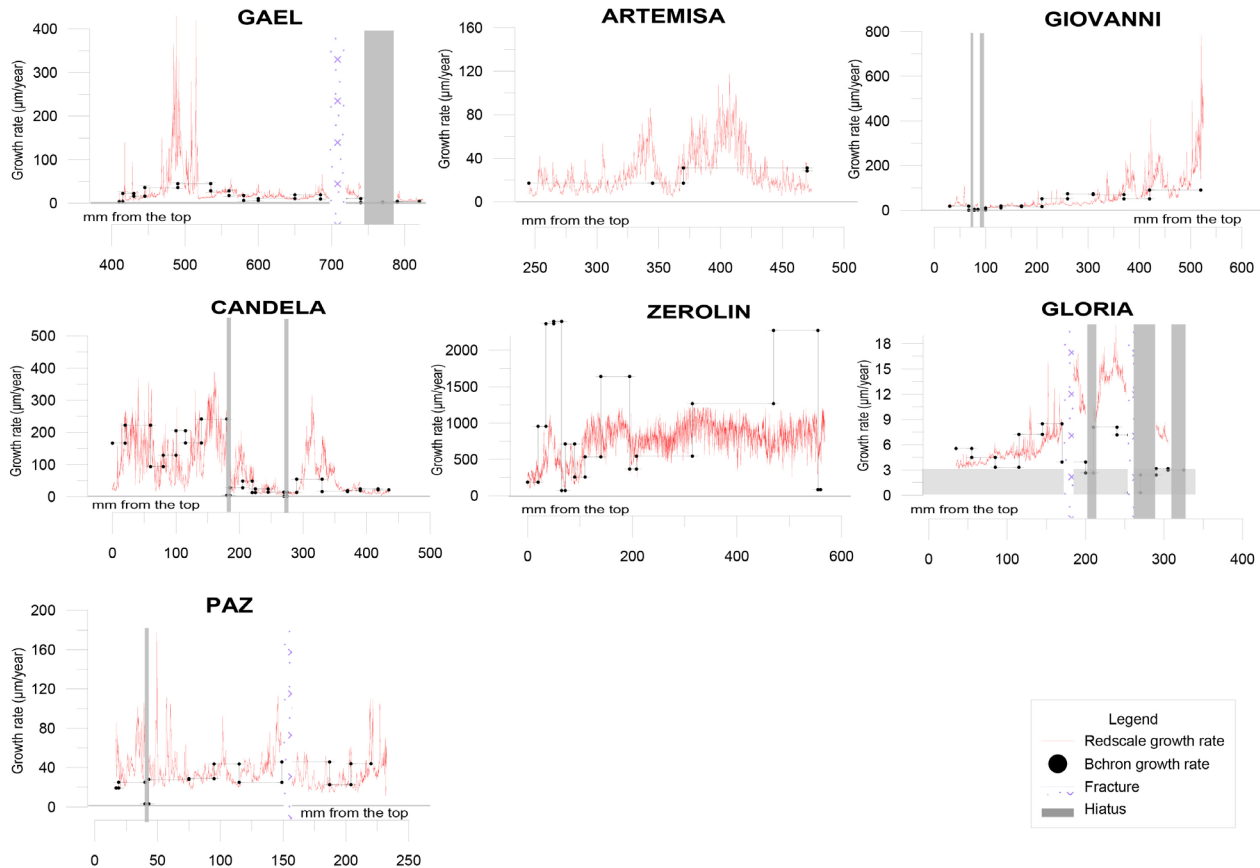


Fig. 7. Comparison between growth rates based on the red continuous color model (red line) and the U-Th derived Bchron model (black dots). Light grey bands indicate fracture in the sample. Dark grey bands indicate suspected growth hiatuses (for interpretation of the references to color in this figure and its legend, the reader is referred to the web version of the article). Comparison between growth rates based on the red continuous color model and the linear interpolation of U-Th dates can be consulted in Supplementary Fig. S4.

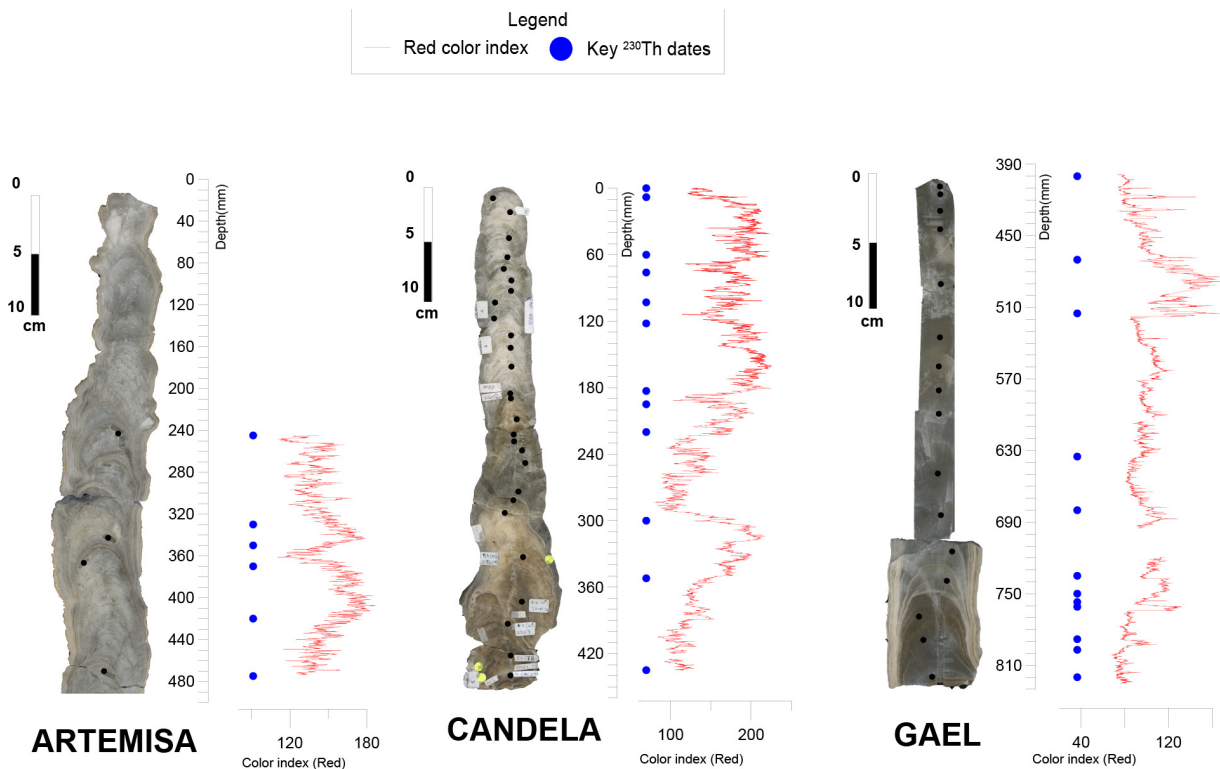


Fig. 8. Suggested placement of sampling location for U-Th dating. Red color index model in 3 stalagmites with corresponding completed U-Th dates (black dots). Locations of where it may be advisable for further dating to capture key growth variability are illustrated by blue dots (for interpretation of the references to color in this figure and its legend, the reader is referred to the web version of the article).

## CONCLUSIONS

Stalagmite color is shown to covary with growth rate in seven stalagmites. For each stalagmite, an exponential relationship between these two variables is observed and the exponent of the function can be tuned to optimize the fit to U-Th derived dates. This finding has two main applications for development of age models from stalagmites. First, prior to any U-Th dating, an initial scan of the polished and wetted stalagmite surface to generate a color index, may be useful in guiding optimal locations of drilling for U-Th dating. This would allow greater efficiency in the selection of samples for dating, which may enable a superior age-depth model to be built with fewer dates. This is extremely important, since one of the major limitations that has been had in this study, and that have limited a better fit of the color model, was the multitude of alterations that the surface of all the stalagmites has suffered (e.g., Gael). Secondly the color index model may be useful for the interpolation of ages between dated points.

Most interpolation algorithms assume constant growth rate between tie points, however, our color analysis, and other laminae counting methods, suggest variations in growth rates occur on a much shorter longitudinal scales than typically dated. In addition, this fitting may be useful to identify U-Th dates which are outliers and unreliable, for example due to non-closed system behavior.

The continuous color index profile is most straightforward on samples with negligible fractures and drilling perforations, i.e., as an initial, and not final, part of stalagmite analysis. We find that the resolution of standard desktop scanners is sufficient for high quality analysis, making this an accessible and useful technique for initial stalagmite analysis. The current study has evaluated a relatively small number of samples, and future studies should assess if these are general relationships, and if the relationship between color and growth rate is universally best approximated by an exponential function, as well as whether this exponential adjustment parameters (or fit parameters in general), are similar across a broad range of stalagmites.

In conclusion, this study has attempted to lay the foundations for the study of the relationship between speleothems coloration and growth rate. Evidence of validity has been found that the exponential function is the one that best describes the relationship between these two variables. However, despite the advantages that an analysis of stalagmite color can provide (e.g., selection of U-Th dates location or enhancement of age models), the current results should be considered with caution as much more research is needed in this line to verify that these relationships can be generalized to stalagmites from other climatic and cave settings.

## ACKNOWLEDGEMENTS

This research was financially supported by OPERA (CTM2013-48639-C2-1-R), University of Oviedo (UNOV-16-RLD-UE-3), PYCACHU (PID2019-106050RB-I00), and the National Natural Science Foundation of

China (NSFC 41888101). We are grateful to A. Martínez (SCTs, Universidad de Oviedo), E. Cabal (Dep. geología, Universidad de Oviedo), J. Guitián, O. Kost and J. Sliwinski (Dpt. of earth sciences, ETH) for their help with the laboratory work. J. Pisonero (Dept. Física, Universidad de Oviedo) and B. Revels (Dpt. of Earth Sciences, ETH) are acknowledged for their help. We thank reviewers for their comments that significantly improved this paper.

Authorship statement: HS conceived the study. HS y CCB designed the study. CCB, AM, MI, HC and RLE performed the measurements. CCB and AGP carried out the analysis and data interpretation. CCB wrote the original draft. All authors were involved in the revision of the original draft.

## REFERENCES

- Barati, R., 2013. Application of excel solver for parameter estimation of the nonlinear Muskingum models. *KSCE Journal of Civil Engineering*, 17, 1139-1148. <https://doi.org/10.1007/s12205-013-0037-2>
- Chalmin, E., Perrette, Y., Fanget, B., Susini, J., 2013. Investigation of organic matter entrapped in synthetic carbonates—a multimethod approach. *Microscopy and Microanalysis*, 19, 132-144. <https://doi.org/10.1017/S1431927612013773>
- Cheng, H., Edwards, R.L., Shen, C.C., Polyak, V.J., Asmerom, Y., et al., 2013. Improvements in  $^{230}\text{Th}$  dating,  $^{230}\text{Th}$  and  $^{234}\text{U}$  half-life values, and U-Th isotopic measurements by multi-collector inductively coupled plasma mass spectrometry. *Earth and Planetary Science Letters*, 371, 82-91. <https://doi.org/10.1016/j.epsl.2013.04.006>
- Cui, Y.F., Wang, Y.J., Cheng, H., Zhao, K., Kong, X.G., 2012. Isotopic and lithologic variations of one precisely-dated stalagmite across the Medieval/LIA period from Heilong Cave, central China. *Climate of the Past*, 8, 1541-1550. <https://doi.org/10.5194/cp-8-1541-2012>
- Dreybrodt, W., 1999. Chemical kinetics, speleothem growth and climate. *Boreas*, 28, 347-356. <https://doi.org/10.1080/030094899422073>
- Drysdale, R.N., Zanchetta, G., Hellstrom, J.C., Fallick, A.E., Zhao, J.X., Isola, I., Bruschi, G., 2004. Palaeoclimatic implications of the growth history and stable isotope ( $\delta^{18}\text{O}$  and  $\delta^{13}\text{C}$ ) geochemistry of a Middle to Late Pleistocene stalagmite from central-western Italy. *Earth and Planetary Science Letters*, 227, 215-229. <https://doi.org/10.1016/j.epsl.2004.09.010>
- Ferreira, T., Rasband, W., 2012. ImageJ user guide. ImageJ/Fiji. <https://imagej.nih.gov/ij/docs/guide/user-guide.pdf>
- Fairchild, I.J., Baker, A., 2012. *Speleothem science: from process to past environments*. Wiley, Oxford, 432 p.
- Frisia, S., 2014. Microstratigraphic logging of calcite fabrics in speleothems as tool for palaeoclimate studies. *International Journal of Speleology*, 44(1), 1-16. <https://digitalcommons.usf.edu/ijs/vol44/>
- Frisia, S., Borsato, A., Fairchild, I.J., McDermott, F., 2000. Calcite fabrics, growth mechanisms, and environments of formation in speleothems from the Italian Alps and southwestern Ireland. *Journal of Sedimentary Research*, 70, 1183-1196. <https://doi.org/10.1306/022900701183>
- Genty, D., Quinif, Y., 1996. Annually laminated sequences in the internal structure of some Belgian

- stalagmites; importance for paleoclimatology. *Journal of Sedimentary Research*, 66, 275-288.  
<https://doi.org/10.1306/D426831A-2B26-11D7-8648000102C1865D>
- Goodwin, L.D., Leech, N.L., 2006. Understanding correlation: Factors that affect the size of r. *The Journal of Experimental Education*, 74, 249-266.  
<https://doi.org/10.3200/JEXE.74.3.249-266>
- Hanrahan, P., Krueger, W., 1993. Reflection from layered surfaces due to subsurface scattering. *Proceedings of the 20th Annual Conference on Computer Graphics and Interactive Techniques*, ACM, 165-174.  
<https://doi.org/10.1145/166117.166139>
- Haslett, J., Parnell, A., 2008. A simple monotone process with application to radiocarbon-dated depth chronologies. *Journal of the Royal Statistical Society: Series C (Applied Statistics)*, 57, 399-418.  
<https://doi.org/10.1111/j.1467-9876.2008.00623.x>
- Hirschey, S.H., 2015. Speleothem formation and composition in hot and cool cave: Assessing the reliability of paleoclimate archives in high CO<sub>2</sub> environments. Unpublished Bachelor Thesis, Wesleyan University, Middletown, 106 p.  
<https://doi.org/10.14418/wes01.1.1185>
- Hössjer, O., 1995. Exact computation of the least trimmed squares estimate in simple linear regression. *Computational Statistics & Data Analysis*, 19, 265-282. [https://doi.org/10.1016/0167-9473\(95\)92697-V](https://doi.org/10.1016/0167-9473(95)92697-V)
- Hu, J., Emile-Geay, J., Partin, J., 2017. Correlation-based interpretations of paleoclimate data—where statistics meet past climates. *Earth and Planetary Science Letters*, 459, 362-371.  
<https://doi.org/10.1016/j.epsl.2016.11.048>
- Hua, Q., McDonald, J., Redwood, D., Drysdale, R., Lee, S., Fallon, S., Hellstrom, J., 2012. Robust chronological reconstruction for young speleothems using radiocarbon. *Quaternary Geochronology*, 14, 67-80. <https://doi.org/10.1016/j.quageo.2012.04.017>
- Kaal, J., Martínez-Pillado, V., Martínez Cortizas, A., Sanjurjo Sánchez, J., Aranburu, A., Arsuaga, J.L., Iriarte, E., 2021. Bacteria, guano and soot: Source assessment of organic matter preserved in black laminae in stalagmites from caves of the Sierra de Atapuerca (N Spain). *International Journal of Speleology*, 50(2), 121-135. <https://doi.org/10.5038/1827-806X.50.2.2382>
- Kaufmann, G., Dreybrodt, W., 2004. Stalagmite growth and palaeo-climate: an inverse approach. *Earth and Planetary Science Letters*, 224, 529-545.  
<https://doi.org/10.1016/j.epsl.2004.05.020>
- Kemp, A.E., Dean, J., Pearce, R.B., Pike, J., 2002. Recognition and analysis of bedding and sediment fabric features. In: Last, W.M., Smol, J.P. (Eds.), *Tracking environmental change using lake sediments*, Vol. 2, Physical and geochemical methods. Springer, Dordrecht, p. 7-22. DOI: 10.1007/0-306-47670-3\_2
- Koffarnus, M.N., Franck, C.T., Stein, J. S., Bickel, W.K., 2015. A modified exponential behavioral economic demand model to better describe consumption data. *Experimental and Clinical Psychopharmacology*, 23(6), 504-512.  
<https://doi.org/10.1037/pha0000045>
- Labuhn, I., Genty, D., Vonhof, H., Bourdin, C., Blamart, D., et al., 2015. A high-resolution fluid inclusion  $\delta^{18}\text{O}$  record from a stalagmite in SW France: modern calibration and comparison with multiple proxies. *Quaternary Science Reviews*, 110, 152-165.  
<https://doi.org/10.1016/j.quascirev.2014.12.021>
- Lachniet, M.S., Bernal, J.P., Asmerom, Y., Polyak, V., 2012. Uranium loss and aragonite-calcite age discordance in a calcitized aragonite stalagmite. *Quaternary Geochronology*, 14, 26-37.  
<https://doi.org/10.1016/j.quageo.2012.08.003>
- Lasdon, L.S., Fox, R.L., Ratner, M.W., 1974. Nonlinear optimization using the generalized reduced gradient method. *Revue française d'automatique, informatique, recherche opérationnelle. Recherche opérationnelle*, 8, 73-103.  
<https://doi.org/10.1051/ro/197408V300731>
- Lewis, S.C., Gagan, M.K., Ayliffe, L.K., Zhao, J.X., Hantoro, W.S., et al., 2011. High-resolution stalagmite reconstructions of Australian-Indonesian monsoon rainfall variability during Heinrich stadial 3 and Greenland interstadial 4. *Earth and Planetary Science Letters*, 303, 133-142.  
<https://doi.org/10.1016/j.epsl.2010.12.048>
- Martrat, B., Grimalt, J.O., Shackleton, N.J., de Abreu, L., Hutterli, M.A., Stocker, T.F., 2007. Four climate cycles of recurring deep and surface water destabilizations on the Iberian margin. *Science*, 317, 502-507.  
<https://doi.org/10.1126/science.1139994>
- Parnell, A.C., Haslett, J., Allen, J.R., Buck, C.E., Huntley, B., 2008. A flexible approach to assessing synchronicity of past events using Bayesian reconstructions of sedimentation history. *Quaternary Science Reviews*, 27, 1872-1885.  
<https://doi.org/10.1016/j.quascirev.2008.07.009>
- Pontes, H.S., Fernandes, L.A., de Melo, M.S., Guimarães, G.B., Massuqueto, L.L., 2020. Speleothems in quartz-sandstone caves of Ponta Grossa municipality, Campos Gerais region, Paraná state, southern Brazil. *International Journal of Speleology*, 49(2), 119-136.  
<https://doi.org/10.5038/1827-806X.49.2.2313>
- Principato, S.M., 2005. X-ray radiographs of sediment cores: a guide to analyzing diamicton. In: Francus, P. (Ed.), *Image analysis, sediments and paleoenvironments*, Springer, Dordrecht, p. 165-185.  
[https://doi.org/10.1007/1-4020-2122-4\\_9](https://doi.org/10.1007/1-4020-2122-4_9)
- Shen, C.C., Edwards, R.L., Cheng, H., Dorale, J.A., Thomas, R.B., Moran, S.B., Weinstein, S.E., Edmonds, H.N., 2002. Uranium and thorium isotopic and concentration measurements by magnetic sector inductively coupled plasma mass spectrometry. *Chemical Geology*, 185, 165-178.  
[https://doi.org/10.1016/S0009-2541\(01\)00404-1](https://doi.org/10.1016/S0009-2541(01)00404-1)
- Smith, A.R., 1978. Color gamut transform pairs. *ACM Siggraph Computer Graphics*, 12, 12-19.  
<https://doi.org/10.1145/965139.807361>
- Stoll, H., Mendez-Vicente, A., Gonzalez-Lemos, S., Moreno, A., Cacho, I., Cheng, H., Edwards, R.L., 2015. Interpretation of orbital scale variability in mid-latitude speleothem  $\delta^{18}\text{O}$ : Significance of growth rate controlled kinetic fractionation effects. *Quaternary Science Reviews*, 127, 215-228.  
<https://doi.org/10.1016/j.quascirev.2015.08.025>
- Stoll, H.M., Moreno, A., Mendez-Vicente, A., Gonzalez-Lemos, S., Jimenez-Sanchez, M., Dominguez-Cuesta, M.J., Edwards, R.L., Cheng, H., Wang, X., 2013. Paleoclimate and growth rates of speleothems in the northwestern Iberian Peninsula over the last two glacial cycles. *Quaternary Research*, 80, 284-290.  
<https://doi.org/10.1016/j.yqres.2013.05.002>
- Tan, L., Cai, Y., Cheng, H., An, Z., Edwards, R.L., 2009. Summer monsoon precipitation variations in central China over the past 750 years derived from a high-resolution absolute-dated stalagmite. *Palaeogeography, Palaeoclimatology, Palaeoecology*, 280, 432-439.  
<https://doi.org/10.1016/j.palaeo.2009.06.030>
- Tesoriero, A.J., Pankow, J.F., 1996. Solid solution

- partitioning of Sr<sup>2+</sup>, Ba<sup>2+</sup>, and Cd<sup>2+</sup> to calcite. *Geochimica et Cosmochimica Acta*, 60, 1053-1063.  
[https://doi.org/10.1016/0016-7037\(95\)00449-1](https://doi.org/10.1016/0016-7037(95)00449-1)
- Thomas, M.E., 2006. Optical propagation in linear media: Atmospheric gases and particles, solid-state components, and water. Oxford University Press, Oxford, 559 p.  
<https://doi.org/10.1093/oso/9780195091618.001.0001>
- Treble, P.C., Chappell, J., Shelley, J.M.G., 2005. Complex speleothem growth processes revealed by trace element mapping and scanning electron microscopy of annual layers. *Geochimica et Cosmochimica Acta*, 69, 4855-4863. <https://doi.org/10.1016/j.gca.2005.06.008>
- Vanghi, V., Borsato, A., Frisia, S., Howard, D.L., Gloy, G., Hellstrom, J., Bajo, P., 2019. High-resolution synchrotron X-ray fluorescence investigation of calcite coralloid speleothems: Elemental incorporation and their potential as environmental archives. *Sedimentology*, 66, 2661-2685.  
<https://doi.org/10.1111/sed.12607>
- Von Gunten, L., Grosjean, M., Rein, B., Urrutia, R., Appleby, P., 2009. A quantitative high-resolution summer temperature reconstruction based on sedimentary pigments from Laguna Aculeo, central Chile, back to AD 850. *The Holocene*, 19, 873-881.  
<https://doi.org/10.1177/0959683609336573>
- Webster, J.W., Brook, G.A., Railsback, L.B., Cheng, H., Edwards, R.L., Alexander, C., Reeder, P.P., 2007. Stalagmite evidence from Belize indicating significant droughts at the time of Preclassic Abandonment, the Maya Hiatus, and the Classic Maya collapse. *Palaeogeography, Palaeoclimatology, Palaeoecology*, 250, 1-17.  
<https://doi.org/10.1016/j.palaeo.2007.02.022>
- Zhao, M., Li, H.C., Liu, Z.H., Mii, H.S., Sun, H.L., Shen, C.C., Kang, S.C., 2015. Changes in climate and vegetation of central Guizhou in southwest China since the last glacial reflected by stalagmite records from Yelang Cave. *Journal of Asian Earth Sciences*, 114, 549-561. <https://doi.org/10.1016/j.jseas.2015.07.021>